Analysis of mobile monitoring data from the microAeth® MA200 for measuring changes in black carbon on the roadside in Augsburg

Xiansheng Liu[1,2], Hadiatullah Hadiatullah[3], Xun Zhang[4,5], L. Drew Hill[6], Andrew H. A. White[6,7], Jürgen Schnelle-Kreis[1], Jan Bendl[1,8], Gert Jakobi[1], Brigitte Schloter-Hai[1], Ralf Zimmermann[1,2]

[1]Joint Mass Spectrometry Centre, Cooperation Group Comprehensive Molecular Analytics, Helmholtz Zentrum München, German Research Centre for Environmental Health, Ingolstädter Landstr. 1, 85764 Neuherberg, Germany

[2]Joint Mass Spectrometry Centre, Chair of Analytical Chemistry, University of Rostock, 18059 Rostock, Germany

[3]School of Pharmaceutical Science and Technology, Tianjin University, 300072 Tianjin, China

[4]Beijing Key Laboratory of Big Data Technology for Food Safety, School of Computer Science and Engineering, Beijing Technology and Business University, 100048 Beijing, China

[5]Key Laboratory of Resources Utilization and Environmental Remediation, Institute of Geographical Sciences and Natural Resources Research, Chinese Academy of Sciences, 100101 Beijing, China

[6]AethLabs, San Francisco, CA, USA

[7]Yale School of Medicine, New Haven, CT, USA

[8]Institute for Environment Studies, Faculty of Science, Charles University, Prague, Czech Republic

Correspondence to: Xun Zhang (zhangxun@btbu.edu.cn); Jürgen Schnelle-Kreis (juergen.schnelle@helmholtz-muenchen.de).

Abstract. The portable microAeth® MA200 (MA200) is widely applied for measuring black carbon in human exposure profiling and mobile air quality monitoring. Due to its relatively new on the market, the field lacks a refined assessment of the instruments performance under various settings and data post-processing approaches. This study assessed the mobile real-time performance of the MA200 to determine a suitable noise reduction algorithm in an urban area, Augsburg, Germany. Noise reduction and negative value mitigation were explored via different data post-processing methods (i.e., local polynomial regression (LPR), optimized noise reduction averaging (ONA), and centered moving average (CMA)) under common sampling interval times (i.e., 5, 10, and 30 s). After noise reduction, the treated-data were evaluated and compared by (1) the amount of useful information attributed to retention of microenvironmental characteristics; (2) relative number of negative values remaining; (3) reduction and retention of peak samples; and (4) the amount of useful signal retained after correction for local background conditions. Our results identify CMA as a useful tool for isolating the central trends of raw black carbon concentration data in real time while reducing non-sensical negative values and the occurrence and magnitudes of peak samples that affect visual assessment of the data without substantially affecting bias. Correction for local background concentrations improved the CMA treatment by bringing nuanced microenvironmental changes into more visible. This analysis employs a number of different post-processing methods for black carbon data, providing comparative insights for

researchers looking for black carbon data smoothing approaches, specifically in a mobile monitoring framework and data collected using the microAeth® series of aethalometers.

Keywords: Black carbon; Mobile measurement; Noise reduction; peak sample; Background correction

1 Introduction

Black carbon particulate matter with size ranging from 0.01 to 1 μm (Zhou et al., 2020), is a pollutant comprised of a range of carbonaceous materials produced by the incomplete combustion of fossil fuel and biomass containing carbon (Goldberg, 1985), and is suspected of exerting significant impact on health (Anenberg et al., 2012; Janssen et al., 2011; Nichols et al., 2013). Black carbon also has an important role in climate systems due to its strong radiative forcing potential (Kutzner et al., 2018, Sadiq et al., 2015). The International Agency for Research on Cancer (IARC) has classified black carbon as a 2B carcinogen, while researchers have linked black carbon exposures to cardiovascular, respiratory, and neurological diseases (e.g., Nichols et al., 2013). However, the high spatial variability of black carbon among small-scale urban blocks is difficult to characterize with existing monitoring networks which typically rely on fixed monitors (Apte et al., 2017), especially for on-road concentrations. Recently, mobile monitoring has been widely applied for the collection of real-time air quality measurements to assess local air quality, and air pollutant exposures (Liu et al., 2020, 2021). This method can improve the spatiotemporal resolution of measurement data in the urban environment and enables the collection of data such as the traffic-related air pollutant concentrations (Liu et al., 2019). Therefore, mobile measurements are favourably used in human exposure studies to quantify individual exposures and to demonstrate the importance of exposure differences in different microenvironments.

Instrument manufacturers in the USA have recently developed a new instrument for measuring black carbon concentrations in a variety of exposure-related contexts, including personal exposure assessment, ambient and vertical profiling, and indoor emissions concentration measuremnts, among others. This instrument, the microAeth® MA200 (MA200; AethLabs, San Francisco, CA, USA), continuously collects aerosol particles on a filter and measures the optical attenuation (ATN) at 5 wavelengths (880, 625, 528, 470, and 375 nm) with a data collection time base as frequent as 1 Hz. This instrument supports the DualSpot® loading compensation method, which corrects the optical loading effect (Virkkula et al., 2007) and provides more additional information about aerosol optical properties. However, the raw data recorded by the MA200 at high frequencies (e.g., 1 Hz) can exhibit noise that obscures nuanced signals surrounding the central tendency of the data, increasing the difficulty of analysis in mobile settings or during rapidly changing micro-environmental characteristics. These negative values usually contain valid information required for noise reduction or smoothing, and so simply removing them may result in bias. Noise reduction of the raw data without direct removal of negative values is thereby recommended to enhance data quality and temporal resolution (Liu et al., 2020). In addition, when the sampling equipment traverses from a highly polluted to a low polluted area, such as a park, the instrument produces strong negative values due to the measurement principle of the instrument and the strength of the pollution gradient between microenvironments. Therefore, the raw black carbon concentrations collected by MA200 need to be post-processed to ensure that researchers can adequately analyse the spatiotemporal distribution of black carbon.

Some progress has been made in the study of black carbon monitoring (Apte et al., 2011; Dons et al., 2012; Cao et al., 2020), however, noise reduction algorithms have not been fully assessed for the new generation of micro-aethalometers and for mobile monitoring contexts. In previous studies, Hagler et al. (2011) and Cheng et al. (2013) evaluated optimized noise reduction averaging (ONA) for post-processing mobile monitoring data. Due to the high spatial heterogeneity of black carbon, the ONA algorithm may ignore important microenvironmental effects and lead researchers to perhaps incorrectly conclude that resolution of microenvironmental source information cannot be determined from their data.

In this study, we aim to determine a suitable noise reduction algorithm for the MA200 aethalometer, starting with ONA, and moving on to two additional smoothing techniques offered by AethLabs in their suite of free online data post-processing (i.e., noise reduction) tools: the local polynomial regression (LPR) and centered moving average (CMA) algorithms. The interpretation accuracy of data analysed and reported upon in black carbon mobile monitoring study can be increased by assessing the relative performance of these post-processing methods to each other and to ONA. The quality of each noise reduction approach was assessed on data collected in an urban environment and post-processed with ONA, LPR, and CMA. Assessment criteria included (1) retention of detailed information attributed to microenvironmental characteristic; (2) relative number of negative values remained; (3) reduction and retention of peak samples; and (4) retention of detailed information on microenvironmental characteristics after background correction.

2 Methods

2.1 Instrumentation

2.1.1 Sampling Equipment

The MA200 measures optical ATN from black carbon on a filter across 5 optical wavelengths: infrared, red, green, blue, and ultra-violet (880, 625, 528, 470, and 375 nm, respectively). A common black carbon metric called "equivalent black carbon" (eBC) is assessed via the 880 nm channel. The detection limit of the MA200 is reported at 30 ng/m^3 eBC under a 5 min time base and 150 mL/min flow rate (SingleSpot™ mode) and with resolution of 1 ng/m^3 (AethLabs, 2018). In mobile monitoring, the MA200 can be used to estimate personal exposure and quantify eBC mass concentrations in different microenvironments. It should be noted that a predecessor instrument to the MA200, the AE51, has demonstrated some sensitivity to mechanical shock during mobile measurements (Cai et al., 2013). When AethLabs took control of manufacturing the AE51, which was originally produced by Magee

Scientific (Berkeley, CA, USA), instrument opto-electronics were redesigned to reduce such sensitivity. Researchers using redesigned AE51 demonstrated only a small effect on data. Supporting this improvement, Cai et al (2013) found evidence of a substantial improvement in data quality related to vibration-related spikes after an equipment upgrade by AethLabs. In addition, there were no major mechanical shocks to or unique vibrational effects on the instrument and no major differences of accelerometer data in the raw data, precluding these as potential confounders on all instruments.

2.1.2 Instruments preparation

In this study, seven MA200 portable black carbon monitors (serial numbers MA200-0051, MA200-0053, MA200-0059, MA200-0060, MA200-0155, MA200-0153, MA200-159) were used simultaneously to measure black carbon levels at the city centre under different interval times (5 s, 10 s, and 30 s). To evaluate the relative performance of MA200, this study analysed black carbon data collected from multiple MA200 devices, identified individually by serial numbers. The instruments were prepared and adjusted in our laboratory before each walk, consisting of "zero" calibration checks, the examination of the MA200 filter cassette, battery, GPS, and memory checks. Flow calibrations were adjusted with a factory-calibrated flow meter (Alicat Scientific, Inc. Tucson, AZ, USA).

Comparative measurements of the MA200 and a stationary Aethalometer (AE33, Magee Scientific, Berkeley, USA) taken approximately 30 to 60 min between walks showed a good agreement (Pearson's r =0.933) (Liu et al., 2021). In addition, it is worth noting that when the AE33 was used for monitoring black carbon at the same time as the MA200, the AE33 was placed in a fixed station, while the MA200 was used outdoors (in the stroller) during the individual walks, which may have presented different relative humidity and temperature values. This condition did not influence the consistency of eBC concentration measured with both instruments. Information about the date, duration, and time resolution (time base) of each MA200 device are summarised in Table 1. To demonstrate the unit-to-unit comparability between the MA200 units, we performed intercomparisons at fixed monitoring stations (Table S1) and during collocated mobile measurements (Fig. S2). No wavelength dependence was observed between different instruments for fixed and mobile monitoring measurements.

Table 1 Measurements of black carbon by different MA200 devices.

Measurement number	Date (dd/mm/yyyy)	Serial number	Start time (hh:mm:ss)	End time (hh:mm:ss)	Time base (s)	Site
1	27/09/2018	MA200-0051	10:29:10	13:38:20	10	Augsburg, Germany
2	15/11/2018	MA200-0059	11:53:42	16:13:12	10	
3	16/11/2018	MA200-0053	11:34:06	16:33:56	10	
4	26/08/2019	MA200-0060	11:01:56	15:44:46	10	
5	21/02/2020	MA200-0155	10:00:10	13:10:00	5	
6	21/02/2020	MA200-0153	10:00:10	13:10:00	10	
7	21/02/2020	MA200-0159	10:00:10	13:10:00	30	

8	24/11/2020	MA200-0059	09:40:57	11:09:07	10	
9	01/12/2020	MA200-0051	13:29:05	15:19:00	5	Munich, Germany
10	18/12/2020	MA200-0051	14:39:30	15:19:30	30	

2.2 Study design and routes

The MA200 instrument is able to measure black carbon in 1 s, 5 s, 10 s, 30 s, 60 s, and 300 s interval times. The 1 s time base exhibits the most challenging interpretation because of low signal to noise ratio especially at low concentrations, which is similar to other optical black carbon monitors (Hagler et al., 2011). Therefore, 1 s measurement resolution may be most useful when sampling in high concentration environments, performing direct emissions testing and requiring high time resolution for the application. However, the eBC average concentration is low in the city centre of Augsburg, Germany, (measured at 2.62 μg/m^3 in winter by Gu, (2012)) thus we did not use the 1 s time base. Moreover, 60 s and 300 s are too long distance for mobile monitoring, which may affect the accuracy of the spatial variation of pollutants, hence both time bases were also not selected in this study. In order to better understand at which interval time of sampling might be most useful in this context – mobile measurements at low eBC concentrations – three MA200 devices were used in parallel to measure eBC concentrations with the interval times of 5 s, 10 s, and 30 s (Measurement numbers 5-7 in Table 1).

To account for the different land-use types of the microenvironments, a fixed walking route within the centre of the city was determined. Wherever possible, the mobile measurements were carried out on the right side of the road simulating people's common habits (driving and walking on the right side in Germany). All walks along the route were conducted on weekdays, with clear skies and calm winds to avoid misrepresentation of typical urban exposure conditions. The route started from Augsburg University of Applied Sciences (UAS) and continued approximately 14 km for 3 h average walking time, passing through different types of land-use to ensure that different microenvironments were represented the entire areas and the validity of the results (Fig. S1). Meanwhile, as performed in our previous study (Liu et al., 2021), we divided the monitoring route into four microenvironment groups in Augsburg, including high traffic flow (H_Traffic, average 500-1000 vehicles/h), medium traffic flow (M_Traffic, average 200-500 vehicles/h), low traffic flow (L_Traffic, average 1-200 vehicles/h), and park area (N_Traffic, average 0 vehicles/h), according to the actual traffic density examined during the daytime and determining from the traffic flow observed by street views.

Briefly, the study consisted of the following phases, (1) collecting raw black carbon data using the sampling instruments (MA200); (2) smoothing the acquired raw black carbon data under different post-processing methods (i.e., noise reduction); (3) comparing the noise reduction data based on the detail of microenvironmental characteristic and number of negative values; (4) following the peak samples identification by the coefficient of variation (COV) and (5) following the background estimation and correction by thin plate regression spline (TPRS); and (6) finally, selecting the best noise reduction approach.

2.3 Post-processing methods

In order to reduce the noise of concentration data obtained using high time resolutions, post-processing algorithms can be used. AethLabs offers tools for applying several noise reduction algorithms (ONA, LPR, and CMA) to MA-series device data on its website (https://aethlabs.com [note: a free account is required]). The relative utility of the different post-processing methods is determined by (1) the ability to perceive nuanced differences between microenvironmental pollution characteristics after noise reduction; (2) the relative number of negative eBC values remaining; (3) the reduction and retention of peak samples; and (4) the ability to perceive nuanced differences between microenvironmental pollution characteristics with the noise-reduced data after background correction.

2.3.1 ONA (optimized noise reduction averaging)

ONA is based on the time series of three parameters in the original observation data, namely the observation time, the original eBC concentration, and the amount of change in optical ATN over time, as specifically described by Hagler et al. (2011). Briefly, a ΔATN threshold is manually set to prevent the algorithm from recalculating eBC until a certain amount of ATN has been detected (e.g., enough black carbon has deposited on the filter to "confidently" calculate an eBC concentration). The aim is to reduce erroneous and spurious estimation by dynamically extending the effective sample time base, hence, there is sufficient ATN to significantly reduce the error effects of instrument noise. This effective time base will be longer in low concentrations than at higher concentrations and, hence, when operating properly, *no* negatives and less eBC noise will be reported. When using the ONA algorithm, this ΔATN threshold needs to be manually assigned. Hagler et al., (2011) implemented a ΔATN threshold of 0.05 to post-process data from a fixed monitoring site by different Aethalometer models (AE21, AE42, and AE51). However, when applied to MA200 data, a ΔATN threshold of 0.05 results in a very smooth curve and may obscure more information than is necessary to provide a usefully smoothed curve. For this reason, a lower ΔATN threshold of 0.01 was selected for the mobile measurement data of our study (Fig. S3).

2.3.2 LPR (local polynomial regression)

The LPR algorithm is a non-parametric tool similar to a moving average, but it operates on polynomial regression rather than simple averaging (Masry, 1996, Breidt and Opsomer, 2000, Kai et al., 2010). In LPR, the number of points across which to smooth must be manually identified. This value should be chosen to balance effective smoothing of the measured values and the sensitivity required to provide spatial resolution in mobile measurements (e.g., the distance over which the average was taken). The distance resolution was chosen at approximately 100 m. Assuming the sampling speed is 1.3 m/s, when the interval time is 5 s, 10 s, and 30 s, the smoothing number of points are 15, 7, and 3, respectively.

2.3.3 CMA (centered moving average)

The CMA algorithm is a smoothing technique used to make the long-term trends of a time series clearer (Easton and McColl, 1997). Unlike a simple moving average, CMA has no shift or group delay in the data processing, as it incorporates data from both before and after the datapoint that is being smoothed. The smoothing number of points was determined as previously described in the LPR algorithm, assuming a sampling speed of 1.3 m/s.

2.4 Comparison analysis after noise reduction approach

2.4.1 The nuance of microenvironmental characteristics and the proportion of negative values.

After post-processing data, the characteristic change of the treated data is used as criterion to select the best method. In this regard, when the treated data provide more detailed microenvironmental characteristics, the data reflect the actual situation of air pollutants and facilitate the identification of pollution sources. However, if microenvironmental trends are less pronounced, it may hinder the identification of the pollution source. Therefore, more detailed microenvironmental features result in more accurate information. In addition, the number of remaining negative values is determined as another criterion to propose the best method. Specifically, the method with the smallest proportion of the negative values is selected as the best method. The proportion of negative values (NV) remaining was calculated as the number of negative values divided by the total sample size.

2.4.2 Peak sample identification

An earlier study by Brantley et al. (2014) compared several methods for identifying and eliminating peak samples in mobile air pollution measurements. These include identifying samples outside of a threshold based on a median produced using road segmentation, an α-trimmed arithmetic average (Van den Bossche et al., 2015), a running coefficient of variation (COV) (Hagler et al., 2012), an estimate of background standard deviation (Drewnick et al., 2012), a running low 25 % quantile (Choi et al., 2012) and 3 times the standard deviation (Wang et al., 2015). The formula for the running method used in this analysis is previously described by Hagler et al. (2012) with minor modification (Eq. 1):

$$COV_t = \frac{\sqrt{\frac{1}{7}\sum_{i=t-3}^{i=t+3}(x_i - \bar{x})^2}}{\bar{x}_{all}} \tag{1}$$

where COV_t is the 70 s sliding COV of the t-th eBC sample under a 10s time base (representing 30 s prior to the sample, the sample, and 30 seconds after the sample), x_i is the i-th eBC sample, $\bar{x}$ is the average of the t-th eBC sample and the three samples before and after it, and $\bar{x}_{all}$ is the average of all eBC data in one experiment. The 99th quantile of the 70 s sliding COV of all eBC data is used as the threshold for determining “peak sample”. The eBC samples that are greater than this threshold are flagged as peak samples along with the eBC samples 3 data points before and after. However, under different time bases (e.g., 5 s, and 30 s), the sliding COV of the t-th black carbon sample is different. Accordingly, the COV equation is required for modification under different time base.

To calculate the reduction of peak samples (RP), the number of peak samples was calculated before and after post-processing data, and the difference value was obtained. Then the change in the number of peak samples was divided by the total number of peak samples before post-processing data. After noise reduction, we compared the reduction and the number of peak samples to further evaluate post-processing methods. In short, if the reduction of peak samples is high, the treated data has a high peak noise reduction without removing the numbers of peak samples. Therefore, the method with high reduction of peak samples and retaining the number of peak samples after post-processing is considered as the better method.

2.4.3 Background estimation and correction

The ability of a processing method to adequately remove the estimated background concentration was used to evaluate which method provides the most useful information related to microenvironmental effects. A noise reduction method that appears to better facilitate background estimation and correction (as described below calculated from noise-reduced data via a defined background estimation and evaluation approach) is assessed to select a better post-processing method.

Background correction methods include the single sample standardization method, the sliding minimum method, the linear regression post-processing method, and the spline (of minimum) regression post-processing method. Brantley et al. (2014) suggests that a thin plate regression spline (TPRS) method can reliably evaluate the background value of mobile measurements, and be used to examine the "useful" information in the noise-reduced data (i.e. non-spurious, non-background pollution trends). Briefly, the TPRS approach includes three steps: first, the noise reduction data of pollutant was processed by a 30 s moving average; second, the results of the 30 s moving average were sequentially processed by the specified time window (i.e., 5 and 10 min), and the position of the minimum sample of pollutant concentration was identified in each window; and finally, thin-plate spline regression was used to fit the sample of minimum pollutant concentration obtained in the previous step, then the background concentration at each time point was obtained.

3 Results and discussion

The average eBC concentrations of raw, ONA-processed, LPR-processed, and CMA-processed data (Measurements 1-10) monitored by all instruments were compared in this study (Table S2). The results show that the three post-processing methods accounted of approximately 1 % bias from the average of raw concentrations (except measurement 5, ONA-processed data at 5 s). This indicates that the average concentration under each post-processing method did not affect the average concentration of the raw unprocessed data.

3.1 Post-processing data under different interval time

As shown in Figure 1, three MA200s were used at the time bases of 5 s, 10 s, and 30 s. The proportion of negative values in the raw data collected under different time base of was 42.1 %, 37.6 %, and 30.5 %, for 5 s, 10 s, and 30 s, respectively (Fig. 1a, Table 2, Fig S4a). Following this, the raw data were processed using ONA, LPR, and CMA (Fig. 1b, 1c, and 1d).

In the 5 s time base, the eBC values changed very rapidly (Fig. 1a), and the ONA processing of the data resulted in only one value (which was negative) (Fig. 1b). Thus, the microenvironmental characteristics of the eBC concentration were not reproduced. We found all ΔATN ($ATN_{t(0)+\Delta t'} - ATN_0$) data were negative in the raw data collected at 5 s, which, according to the ONA method described above, resulted in only a single value. In short, after the first measurement, the ΔATN threshold (which is positive) for calculating the next value was never reached. The first value was likely a negative value due to a combination of instrument noise, coincidence, and a low background concentration (i.e., low baseline instrument signal), which is consistent with both the raw data measurements and the typical low eBC concentrations in the city centre of Augsburg, Germany (Gu, 2012). It is unclear why ΔATN remained negative, but, given the long series of low concentration vales at the beginning of the sampling and the initial negative measurement, it is possible that the summed ΔATN became increasingly negative as a result of the initial negative ΔATN measurement. The subsequent measurements at low-concentration did not exceed the magnitude of the initial negative ΔATN value. Under these conditions, a cumulative negative sum of ΔATN would prevent the positive ΔATN threshold from being achieved at all. If true, this condition highlights one potential weakness of the ONA algorithm, such as difficulty registering a signal under low concentrations and requires further investigation of the conditions under which ONA is truly unbiased. The observed event prevented the use of ONA in the 5 s time base (Fig. 1b). Previous studies in which ONA was successfully applied implemented a 1 s time base (Hagler et al., 2011; Van den Bossche et al. 2015). After post-processing with LPR and CMA, the microenvironmental characteristics retained more detailed information of the eBC concentration. Further comparison of their negative values revealed that the remaining negative values comprised 28.1 % and 22.9 % of the dataset for LPR and CMA, respectively, after post-processing.

In the 10 s interval time base, negative values were not found after ONA processing, suggesting that a reasonable smoothing effect is obtained at low black carbon concentration. The microenvironmental characteristic presented strong changes against the raw data, remaining less detailed information of air pollution. After post-processing with LPR and CMA, the microenvironmental characteristics revealed more detailed information of air pollution, with 30.2 % of negative values for LPR and 25.3 % for CMA. In the 30 s interval time base, the negative values comprised 0 % of the post-processed data for ONA, 25.5 % for LPR, and 22.4 % for CMA. The 30 s interval dataset presented the lowest proportion of negative values before and after post-processing, due to the longer interval times of sampling. However, the longer 30 s measurement period results in more distance covered during each measurement, given the mobile nature of the sampling device. Thus, 30 s black carbon measurements may be too long to detect local concentration peaks in urban contexts that supported another study (Kerckhoffs et al., 2016).

The ONA algorithm showed a strong tendency to remove negative values and, depending on the ΔATN threshold employed by the user, can remove potentially meaningful low peaks. As a result, the ONA-treated data may present bias that obscure nuanced microenvironmental trends (Fig. 1b). Interestingly, LPR and CMA post-processing are capable of decreasing negative values while retaining microenvironmental trends. Both methods are promising for the analysis of spatiotemporal changes in pollutant concentrations with sensitivity to local sources. Previous studies have shown that the spatiotemporal variability of black carbon is highly heterogeneous (Liu et al., 2019; Liu et al., 2021); the ability to capture spatiotemporal variability of microenvironments is critical for assessing differential exposures among populations.

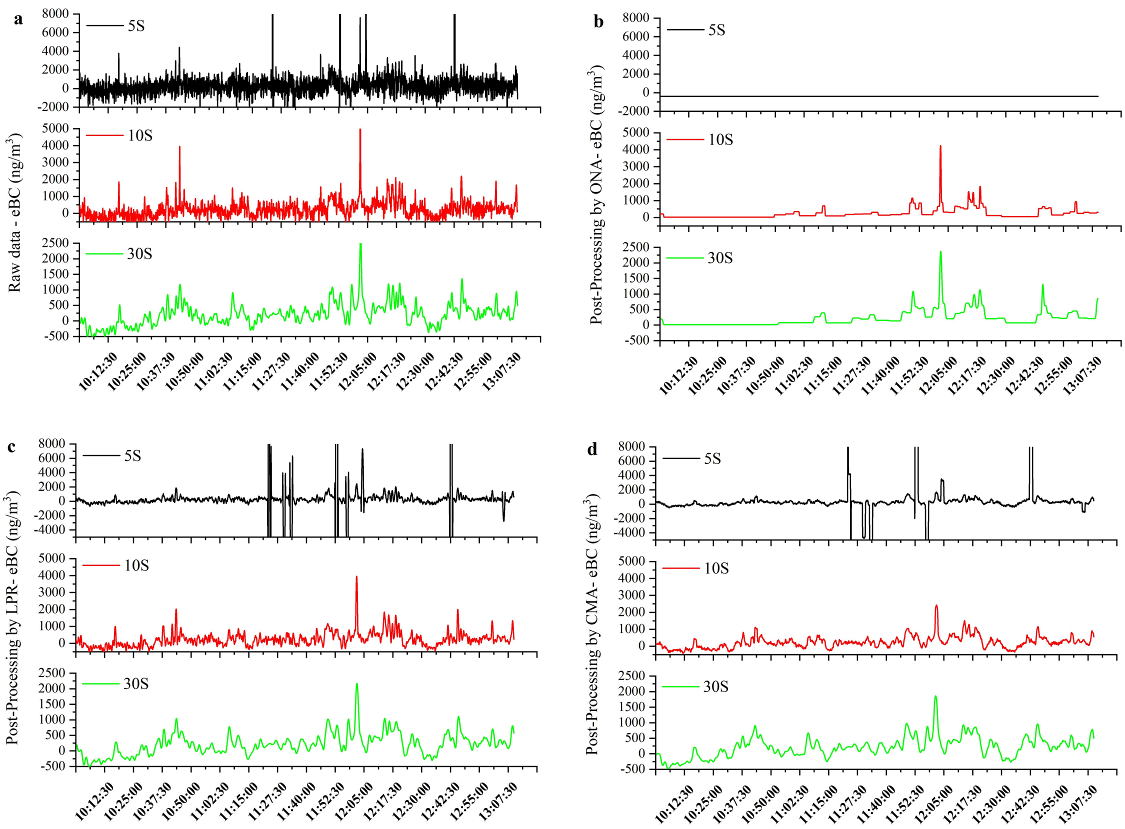

Figure 1 The temporal fluctuations of the black carbon levels measured with the MA200 at sampling time bases of 5 s, 10 s, and 30 s during a typical sampling period (about 190 min), **(a)**, raw data without noise reduction, **(b)**, data treated with optimized noise reduction averaging, **(c)**, data treated with local polynomial regression, and **(d)**, data treated with centered moving average. The analysis was carried out on data streams from three MA200s all collected during a single sampling run (Measurements 5, 6 and 7).

Table 2 The proportion of negative values and average reduction of peak samples under the different post-processing methods (values are shown as (%), NV [%]: Proportion of negative values remained, RP [%]: Average reduction of peak samples. -, no data, measurements 1-10).

Interval time	Factor	RAW	ONA	LPR	CMA
5 s	NV	42.1	-	28.1	22.9
	RP	0	100	72.0	87.4
10 s	NV	37.6	0	30.2	25.3

	RP	0	5.54	22.3	47.7
30 s	NV	30.5	0	25.5	22.4
	RP	0	0.62	6.24	39.1

3.2 Reduction and number of peak samples after post-processing methods

The processing of peak sample is a pivotal evaluation index for the measurement of time-averaged roadside air quality. Passing vehicles, for example, may bias estimates of typical local concentrations due to their contribution to the dataset of peak concentrations that may substantially related to arithmetic averages. Therefore, after noise reduction, we compare the reduction and the retained number of peak samples to further evaluate the post-processing methods.

In the interval time 5 s, the average reduction of peak samples (RP) for the LPR and CMA algorithms was 72.0 % and 87.4 %, respectively (as discussed above, the ONA method could not be used). In this interval time, the reduction of peak samples was relatively high, indicating that when monitoring black carbon at low concentrations and high sample frequencies, drastic noise may occur in the raw data, and higher noise reduction may affect the actual values. Therefore, a suitable interval time should be considered when monitoring low eBC concentrations. In the interval time 10 s, the average reduction of peak samples for the CMA (47.7 %) is higher than ONA (5.54 %) and LPR (22.7 %). In the interval time 30 s, CMA presented the greatest average reduction of peak samples (39.1 %) compared to ONA (6.24 %) and LPR (0.62 %) (Table 2, Fig. S4b). The retention of peak samples remaining after post-processing was also assessed using the COV method (Measurements 1-10). The result showed that all three algorithms retained all peak samples before and after post-processing. In this regard, CMA retained all peak samples despite the highest reduction in their magnitude. Therefore, CMA highlights microenvironmental trends while preserving the identity of peak samples, facilitating the identification of local pollution sources, and may thus be a better post-processing method than ONA or LPR (Table 2, Fig. S4b).

To further characterise the distribution of peak sample concentration under CMA, we performed an intensive graphical analysis on a single data stream (Measurement 4; Fig. 2). As shown in Figure 2, eBC values along the main roads and intersections were higher than other locations, presumably due in large part to stop-and-go traffic and cars in close proximity to the mobile monitor (Fig. 2). It can be seen from Figure 2a that the peak samples of black carbon were mainly found in 4 locations, represented by red triangles. Vehicle counts and traffic in these locations vary depending on the time of measurement. The highest eBC values were repeatedly found in the streets with moderately high traffic volumes and dense coverage with relatively high buildings (street canyon situation), indicating that heterogeneity in air pollution concentrations in Augsburg and similar settings is largely caused by a combination of effects from traffic and topography (Buonanno et al., 2011). To determine whether peak samples are due to local sources or instrumental artefacts, and to provide further evidence that traffic and topography effects are primary contributors to spatial heterogeneity in pollution concentrations, we compared the data measurements of the three collocated MA200 units during

Measurements 5, 6, and 7. The results showed that there were no major differences in the hot spot areas (an indicator of considerable peak samples) identified by the measurements of the three instruments (Fig. S5).

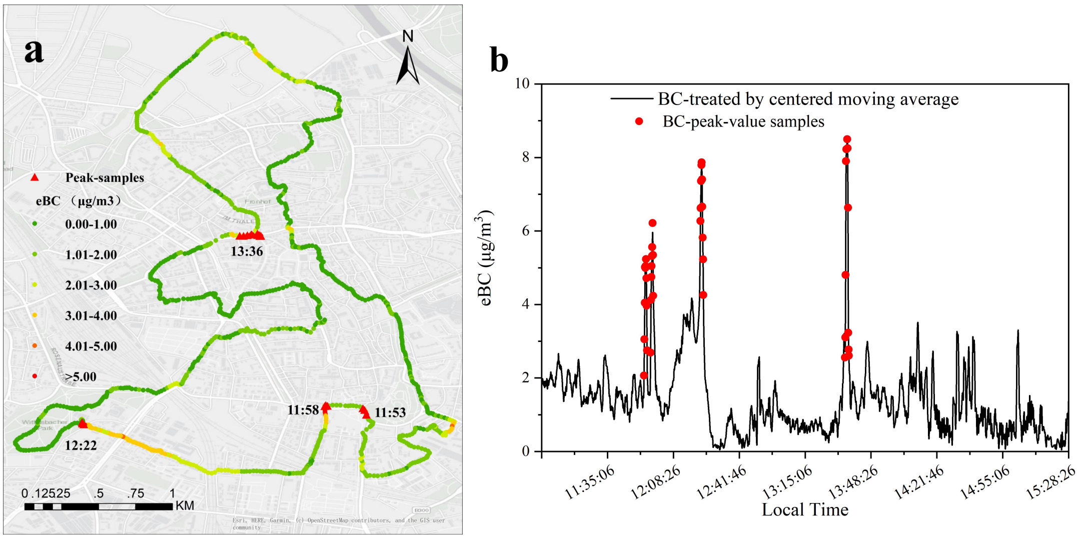

Figure 2 Identification of the spatial **(a)** and temporal **(b)** distribution characteristics of black carbon peak samples based on the coefficient of variation method (the analysis based on measurement 4), © OpenStreetMap contributors. Distributed under a Creative Commons BY-SA License.

3.3 Comparison of background estimation and correction after noise reduction

Local air pollution can be highly affected by long-range and regional transport. The timing and magnitude of such transports vary in space and time and are highly dependent upon the stochasticity of meteorology. As a result, local background concentration changes may vary, affecting the comparability of measurements made at the same location at different times (Brantley et al., 2014). For this reason, reliable comparison of time-variable mobile measurements across a city (and thus reliable pinpointing of hotspots and pinpointing of key local sources) requires effective methods to estimate, isolate, and remove the effects of fluctuations in background concentration. Our analysis indicates that the effectiveness of background correction is affected by the noise reduction method chosen during post-processing.

After post-processing, the data were evaluated using the TPRS method. We calculated the 5 min and 10 min background concentrations under different post-processing approaches. As shown in Figures 3a and b, the background concentration after LPR processing has both the largest proportion of negative values and the most negative values (i.e. negative values of the greatest absolute magnitude), resulting in estimates of background-corrected concentrations that are greater than actual monitored concentrations. Background concentrations calculated after ONA and CMA post-processing presented fewer and lower negative values than LPR, but were not convincingly different from each other. Therefore, to further compare the ONA and CMA algorithm, we also compared concentrations after background correction (Fig. 3c and d). As shown in Figures 3c and d, when the concentration is lower than 1 μg/m^3, the background-corrected results after the ONA processing are smoother than after CMA. This result dampens the signal of local pollutant sources, resulting in a lower utility of post-processed data.

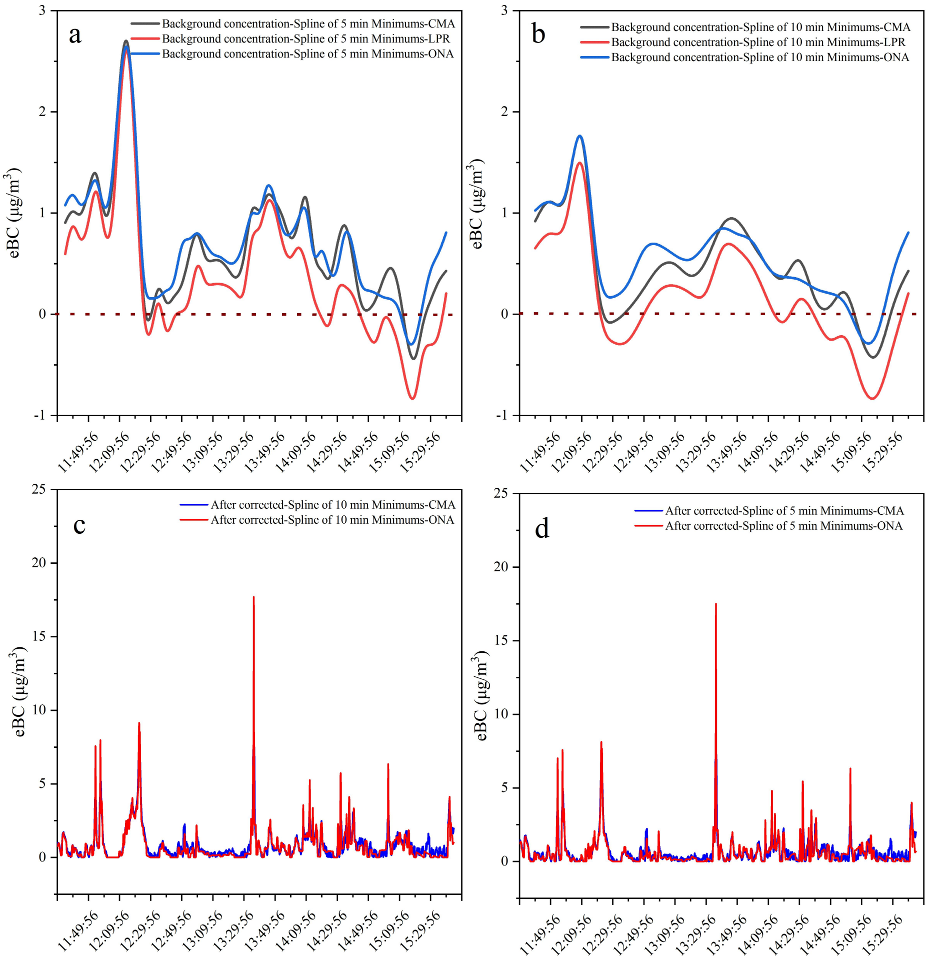

Figure 3 Background concentration of black carbon under different time-series :**(a)**, spline of 5 min minimums, (b), spline of 10 min minimums; and background correction of black carbon under different time-series **(c)** spline of 5 min minimums; (d), spline of 10 min minimums. Analyses are based on Measurement 4.

In order to verify the CMA applicability and its advantages, this study further analysed the eBC concentrations measured by a fixed background monitoring station at the University of Applied Sciences (UAS) (Fig. S6) (Cyrys et al., 2006). The background value under the 5 min window exhibits wave-like characteristics, and the fitting curve in the 10 min window is relatively smooth. However, the TPRS-based background value often does not fluctuate greatly over short periods, and the black carbon background value curve under the 5 min window does not conform to the “actual” urban background situation as estimated using the fixed-site monitor data, which are assumed to primarily represent the fluctuations in background concentrations. Moreover, by comparing the curve produced by the spline of 10 min minimums with the eBC background concentration (Background-UAS, Fig. S6), it can be found that the background correction method based on the time series can well characterize the time-varying characteristics of background pollution in each experiment, suggesting that, of the two options, 10 min showed the better window for fitting the background value curve of black carbon.

Under the TPRS method, the background concentration of eBC can be fitted at any sampling time. The TPRS-estimated background contribution of the observed eBC concentration averaged 37.8 % of the total measured concentration. However, when the contribution of background concentration to a single measurement was examined, a large fluctuation (10.4 -71.3 %) was observed, which may be closely related to sizeable changes in the meteorological conditions, traffic conditions along the road (and over time at the same point in the road), and urban street canyon effects in each measurement. Therefore, based on the comparison of background correction, the CMA showed better applications for estimating the background concentration and location source contribution.

3.4 Generalizability

To verify the generalizability of our assessment, we performed another three measurement runs in Munich (Measurement 8, 9, 10). Raw data were post-processed for noise reduction using CMA (Fig. S7). The results showed that the following method is equally applicable in a city like Munich as in our study site in Augsburg, two cities that differ in location and environmental characteristics (e.g., population, economy, traffic density etc.). After treated by CMA, the peak samples can be identified in different interval times (Fig. S8), and the estimated background concentrations showed few negative values (Fig. S9). Further research into the transferability of our results to a more diverse set of contexts is still needed.

3.5 Practical implications

The MA200 is widely used to measure human exposure to black carbon and for mobile air quality monitoring. In this study the MA200 were applied in mobile measurements in an urban area (Augsburg), and the sensitivity of the final analysis to various data post-processing methods was investigated. In contrast to our findings, Hagler et al., (2011) suggested the use of the ONA algorithm to post-process Aethalometer data from microAeth AE51, portable AE42, and rackmount AE21 aethalometers (Magee Scientific, Berkeley, CA, USA). In their analysis, ONA demonstrated a strong noise reduction in all datasets and retained spatiotemporal variation. ONA also reduced the occurrence of negative data values in low concentration sampling environments. However, for the microAeth® series of black carbon monitoring instruments, our study showed that ONA under reasonable delta ATN thresholding may lead to a considerable dampening of spatiotemporal resolution in local black carbon signals at street level - an effect that is lower under CMA post-processing.

In addition, our analysis highlights that the selection of an appropriate data post-processing method is crucial to the proper assessment and interpretation of exposure-relevant microenvironmental contributors to pollution concentrations in urban areas. This analysis is important when estimating exposures that occur during transit, where spatiotemporal variability in pollution concentrations is vast, like in commuter traffic (Snyder *et al.*, 2013). Due to the typically low-but-heterogeneous nature of eBC concentrations in many areas like Augsburg, noisy measurement with the MA200 under high-frequency sampling may obscure actual trends in measured values. This study demonstrated that post-processing MA200 data using CMA can reliably extract the actual signals from such noise and, alternatively, that post-processing via ONA and LPR could be less reliable. Future researchers and agencies may find a distillation of our results in the form of the flow diagram in Scheme 1 useful in determining how to reliably assess spatiotemporal variability of MA200 measurements for black carbon in different microenvironments.

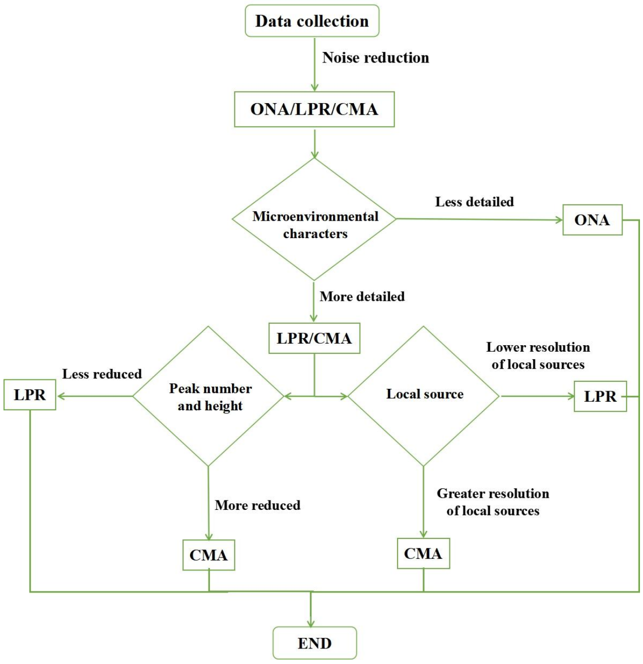

Scheme 1 The proposed decision tree for mobile monitoring data from the microAeth® MA200.

4 Conclusion

A mobile monitoring campaign was conducted in the city centre of Augsburg, Germany to determine a suitable noise reduction algorithm for the MA200 aethalometer. Our results showed that, at the interval time of 5 s, 10 s, and 30 s, CMA post-processing effectively removed spurious negative concentrations without major bias and reliably highlighted effects from local sources, effectively increasing spatiotemporal resolution in mobile measurements. Evaluation of the effects of each method on peak sample reduction and the estimation of background concentrations further support the reliability of the CMA. Further analysis is needed to understand how well these findings apply in different seasons; across different diurnal patterns; and in more-rural, more-urban, and non-German locations.

Data availability

The data are available upon request by contacting the first author of the paper.

Author contribution

X.L: Data curation, Methodology, Software, Writing original draft. H.H: Methodology, Writing original draft. X.Z: Funding acquisition, Project administration. L. DH: Discussion, Writing review & editing. J.SK: Investigation, Supervision. J.B and G.L: Methodology. A. HAW and B.SH: Writing review & editing. RZ: Investigation.

Competing Interest

L. Drew Hill is an employee of AethLabs (San Francisco, CA, USA) and Andrew H.A. White was, at the time of contribution, an intern at AethLabs. These affiliations did not affect the conclusions of the paper.

Acknowledgement

We gratefully thank Erik Hopp (AethLabs, San Francisco, CA, USA) for the implementation and maintenance of the AethLabs data processing web tool.

Financial support

The work is funded by the Germany Federal Ministry of Transport and Digital Infrastructure (BMVI) as part of SmartAQnet (grant No.19F2003B), and by the Research Project of Ministry of Science and Technology of China (2019YFC0507800) and Support Project of High-level Teachers in Beijing Municipal Universities in the Period of 13th Five - year Plan (CIT&TCD201904037).

References

AethLabs. : MicroAeth® MA Series MA200, MA300, MA350 Operating Manual. December 2018, rev 03. Retrieved from https://aethlabs.com/sites/all/content/microaeth/maX/MA200%20MA300%20MA350%20Operating%20Manual%20Rev%2003%20Dec%202018.pdf. Available , April 5, 2021.

Anenberg, S. C., Schwartz, J., Shindell, D., Amann, M., Faluvegi, G., Klimont, Z., ... and Ramanathan, V.: Global air quality and health co-benefits of mitigating near-term climate change through methane and black carbon emission controls. Environmental health perspectives, 120(6), 831-839. https://doi.org/10.1289/ehp.1104301, 2012.

Apte, J. S., Kirchstetter, T. W., Reich, A. H., Deshpande, S. J., Kaushik, G. C. A., Marshall, J, D., and Nazaroff, W. W.: Concentrations of fine, ultrafine, and black carbon particles in auto-rickshaws in New Delhi, India, Atmos. Environ, 45, 4470-4480, https://doi.org/10.1016/j.atmosenv.2011.05.028, 2011

Apte, J. S., Messier, K. P., Gani, S., Brauer, M., Kirchstetter, T. W., Lunden, M. M., Maeshall, J. D., Portier, C. J., Vermeulen, R. C. H., and Hameurg, S. P.: High-Resolution Air Pollution Mapping with

Google Street View Cars. Exploiting Big Data, Environ. Sci. Technol., 12, 6999-7008, https://doi.org/10.1021/acs.est.7b00891, 2017.

Brantley, H., Hagler, G., Kimbrough, S., Williams, R., Mukerjee, S., and Neas, L.: Mobile air monitoring data-processing strategies and effects on spatial air pollution trends, Atmos. Meas. Tech., 7, 2169-2183, https://doi.org/10.5194/amt-7-2169-2014, 2014.

Breidt, F. J. and Opsomer. J. D.: Local polynomial regression estimators in survey sampling. Annals of Statistics 28, 1026-1053, https://www.jstor.org/stable/2673953, 2000.

Buonanno, G., Fuoco, F. C., and Stabile, L.: Influential parameters on particle exposure of pedestrians in urban microenvironments, Atmos. Environ, 7, 1434-1443, https://doi.org/10.1016/j.atmosenv.2010.12.015, 2011.

Cai, J., Yan, B., Kinney, P. L., Perzanowski, M. S., Jung, K. H., Li, T., ... Chillrud, S. N.: Optimization approaches to ameliorate humidity and vibration related issues using the microAeth black carbon monitor for personal exposure measurement. Aerosol Science and Technology, 47(11), 1196-1204. doi: 10.1080/02786826.2013.829551, 2013.

Cao, R., Li, B., Wang, H. W., Tao, S., Peng, Z. R., and He, H. D.: Vertical and Horizontal Profiles of Particulate Matter and Black Carbon Near Elevated Highways Based on Unmanned Aerial Vehicle Monitoring, Sustainability 12, 1204, https://doi.org/10.3390/su12031204, 2020.

Chiliński, M. T., Markowick, K. M., and Kubicki, M.: UAS as a Support for Atmospheric Aerosols Research: Case Study, Pure Appl. Geophys., 9, 3325-3342, https://doi.org/10.1007/s00024-018-1767-3, 2018.

Choi, W., He, M., Barbesant, V., Kozawa, K. H., Mara, S., WIiner, A. M. Paulosn, and S. E.: Prevalence of wide area impacts downwind of freeways under pre-sunrise stable atmospheric conditions, Atmos. Environ, 62, 318-327, https://doi.org/10.1016/j.atmosenv.2012.07.084, 2012.

Cyrys, J., Pitz, M., Soentgen, J., Zimmermann, R., Wichmann, H. E., and Peters, A.: New Measurement Site for Physical and Chemical Particle Characterization in Augsburg. Germany, Epidemiology (Cambridge, Mass.) 17, S250-S251, 2006.

Dons, E., Int Panis, L., Van Poppel, M., Theunis, J., and Wets, G.. Personal exposure to Black Carbon in transport microenvironments, Atmos. Environ, 55, 392-398, https://doi.org/10.1016/j.atmosenv.2012.03.020, 2012.

Drewnick, F., Böttger, T., Von Der Weiden-Reinmüller, S. L., Zorn, S. R., Klimach, T., Schneider, J., and Borrmann, S.: Design of a mobile aerosol research laboratory and data processing tools for effective stationary and mobile field measurements, Atmos. Meas. Tech, 5(6), 1443-1457, https://doi.org/10.5194/amtd-5-2273-2012, 2012.

Easton, V. J., and McColl, J. H.: Statistics Glossary v1.1, 1997.

Gu, J., 2012. Characterizations and sources of ambient particles in Augsburg. Germany.

Hankey, Steve. Exposure to particulate air pollution during active travel. Retrieved from the University of Minnesota Digital Conservancy, https://hdl.handle.net/11299/182828, 2014.

Hagler, G. S. W., Lin, M., Khlystov, A., Baldauf, R. W., Isakov, V., Faircloth, J., and Jackson, L. E.: Field investigation of roadside vegetative and structural barrier impact on near-road ultrafine particle concentrations under a variety of wind conditions, Sci. Total Environ., 416, 7-15, https://doi.org/10.1016/j.scitotenv.2011.12.002, 2012

Hagler, G.S., Yelverton, T.L., Vedantham, R., Hansen, A.D. and Turner, J.R.: Post-processing Method to Reduce Noise while Preserving High Time Resolution in Aethalometer Real-time Black Carbon Data, Aerosol Air Qual. Res. 11: 539-546. https://doi.org/10.4209/aaqr.2011.05.0055, 2011.

IARC 2012: Diesel and Gasoline Engine Exhausts and Some Nitroarenes, IARC Monographs on the Evaluation of Carcinogenic Risks to Humans Volume 105, ISBN 978-92-832-1210-2. 2012.

Janssen, N. A., Hoek, G., Simic-Lawson, M., Fischer, P., Van Bree, L., Ten Brink, H., ... and Cassee, F. R.; Black carbon as an additional indicator of the adverse health effects of airborne particles compared with PM10 and PM2. 5. Environmental health perspectives, 119(12), 1691-1699. https://doi.org/10.1289/ehp.1003369, 2011.

Kai, B., Li, R., Zou, H. Local composite quantile regression smoothing: an efficient and safe alternative to local polynomial regression. Journal of the Royal Statistical Society: Series B (Statistical Methodology), 72(1), 49-69. https://doi.org/10.1111/j.1467-9868.2009.00725.x, 2010

Kerckhoffs, J., Hoek, G., Messier, K. P., Brunekreef, B., Meliefste, K., Klompmaker, J. O., Vermeulen, R. Comparison of ultrafine particle and black carbon concentration predictions from a mobile and short-term stationary land-use regression model. Environmental science & technology, 50(23), 12894-12902. https://doi.org/10.1021/acs.est.6b03476, 2016.

Kutzner, R. D., von Schneidemesser, E., Kuik, F., Queddenau, J., Weatherhead, E. C., and Schamle, J.: Long-term monitoring of black carbon across Germany, Atmos. Environ, 185, 41-52, https://doi.org/10.1016/j.atmosenv.2018.04.039, 2018.

Liu, M., Peng, X., Meng, Z., Zhou, T., Long, L., She, Q. Spatial characteristics and determinants of in-traffic black carbon in Shanghai, China: Combination of mobile monitoring and land use regression model. Sci. Total Environ., 658, 51-61, https://doi.org/10.1016/j.scitotenv.2018.12.135, 2019.

Liu, X., Schnelle-Kreis, J., Zhang, X., Bendl, J., Khedr, M., Jakobi, G., Schloter-Hai, B., Hovorka, J., and Zimmermann, R.: Integration of air pollution data collected by mobile measurement to derive a preliminary spatiotemporal air pollution profile from two neighboring German-Czech border villages. Sci. Total Environ., 722, 137632, https://doi.org/10.1016/j.scitotenv.2020.137632, 2020.

Liu, X., Zhang, X., Schnelle-Kreis, J., Jakobi, G., Cao, X., Cyrys, J., ... and Khedr, M.: Spatiotemporal Characteristics and Driving Factors of Black Carbon in Augsburg, Germany: Combination of Mobile Monitoring and Street View Images. Environ. Sci. Technol., https://doi.org/10.1021/acs.est.0c04776, 2021.

Masry, E.: Multivariate local polynomial regression for time series: uniform strong consistency and rates, J. Time Ser. Anal., 17, 571-599, https://doi.org/10.1111/j.1467-9892.1996.tb00294.x, 1996.

Nichols, J. L., Owens, E. O., Dutton, S. J., & Luben, T. J. Systematic review of the effects of black carbon on cardiovascular disease among individuals with pre-existing disease. International journal of public health, 58(5), 707-724. DOI 10.1007/s00038-013-0492-z. 2013.

Sadiq, M., Tao, W., Tao, S., and Liu, J.: Air quality and climate responses to anthropogenic black carbon emission changes from East Asia, North America and Europe, Atmos. Environ., 120, 262-276, https://doi.org/10.1016/j.atmosenv.2015.07.001, 2015.

Van den Bossche, J., Peters, J., Verwaeren, J., Botteldooren, D., Theunis, J., and De Baets, B.: Mobile monitoring for mapping spatial variation in urban air quality: Development and validation of a methodology based on an extensive dataset. Atmos. Environ., 105, 148-161, https://doi.org/10.1016/j.atmosenv.2015.01.017, 2015.

Virkkula, A., Mäkelä, T., Hillamo, R., Yli-Tuomi, T., Hirsikko, A., Hämeri, K., and Koponen, I. K.: A simple procedure for correcting loading effects of aethalometer data. J. Air. Waste. Manag. Assoc., 57(10), 1214-1222, https://doi.org/10.3155/1047-3289.57.10.1214, 2007.

Wang, Z., Lu, F., He, H., Lu, Q., Wang, D., Peng, Z.: Fine-scale estimation of carbon monoxide and fine particulate matter concentrations in proximity to a road intersection by using wavelet neural network with genetic algorithm, Atmos. Environ., 104, 264-272, https://doi.org/10.1016/j.atmosenv.2014.12.058, 2015.

Zhou, H., Lin, J., Shen, Y., Deng, F., Gao, Y., Liu, Y., Dong, H., Zhang, Y., Sun, Q., Fang, J., Tang, S., Wang, Y., Du, Y., Cui, L., Ruan, S., Kong, F., Liu, Z., and Li, T.: Personal black carbon exposure and its determinants among elderly adults in urban China. Environment International, 138, 105607, https://doi.org/10.1016/j.envint.2020.105607, 2020.